Journal of Energy Storage 45 (2022) 103767

Contents lists available at ScienceDirect

Journal of Energy Storage

journal homepage: www.elsevier.com/locate/est

Research Papers

A multi-factor evaluation method for the thermal runaway risk of lithium-ion batteries

Zhirong Wang [a,*], Shichen Chen [a], Xinrui He [b], Chao Wang [b], Dan Zhao [a]

[a] Jiangsu Key Laboratory of Hazardous Chemicals Safety and Control, College of Safety Science and Engineering, Nanjing Tech University, Nanjing 211816, China
[b] Clean Energy Materials and Engineering Center, State Key Laboratory of Electronic Thin Film and Integrated Device, School of Electronic Science and Engineering, University of Electronic Science and Technology of China, Chengdu 611731, China

ARTICLE INFO

Keywords:
Lithium-ion battery
Thermal runaway
Risk assessment
Fuzzy analytic hierarchy process

ABSTRACT

To systematically and quantitatively establish a multi-factor evaluation method for the thermal runaway risk of lithium-ion batteries (LIBs), the fuzzy analytic hierarchy process was adopted in this paper. The own hazardous factor of battery, hazardous factor of vented gases, jet fire and high-temperature mixture (JFHM), ejected powder and their corresponding sub-factors were evaluated and analyzed. Combined with literature, the model of multi-factor evaluation method was established and the index system was determined. The pair-wise comparison matrixes for the thermal runaway risk were drawn, the triangular fuzzy method was used to calculate and the evaluation weight was obtained. The factors' ranges of the criteria risk grades were quantitatively determined. The risk of thermal runaway consequences under the selected abuse condition was analyzed with a case study. The result shows that the thermal runaway risk from LIBs under the selected abuse condition is level III: the LIB is more dangerous after thermal runaway. Meanwhile, in this method, the lower explosion limit of gas and the maximum height/ length of the JFHM are the two factors with the greatest weights. In the actual design and use process, people should pay attention to the protection of the runaway gas explosion and the harm of JFHM.

1. Introduction

With the development of new energy vehicles using lithium-ion batteries (LIBs) as a power source, the requirements for the density of energy [1,2] are getting higher and higher. However, safety issues are becoming more prominent. Increasing the capacity will increase the risk of LIBs [3]. The danger of LIBs mainly comes from the thermal runaway [4] that occurs when they are abused, with hazardous behaviors such as high temperature, flames, ejected products, etc.

For the risk assessment of LIBs, the current focus is mainly on establishing standards to set test items and detection methods to test the related risks of LIBs. For example, Ashtiani [5] developed a method to evaluate the dangers of batteries. It combined the extreme abuse conditions that the battery may be in and the use of safety protection devices to determine its risk value. Soares et al. [6] proposed a detailed risk analysis method for LIBs in a stationary state, studied the risks of a variety of hazards and dangerous states, and put forward a targeted safety management method to reduce the probability and severity of danger. The above analysis methods all analyze the dangers of LIBs from different conditions and situations, but they lack quantitative and systematic analysis. Therefore, there is an urgent need for a method that can quantitatively and systematically analyze the dangers of LIBs, and the use of analytic hierarchy process (AHP) [7] can achieve this goal in a targeted manner.

The thermal runaway risk of LIBs is affected by many parameters, including the own factors of battery (high temperature, time to thermal runaway, etc.), factors of thermal runaway vented gases (Flammability and explosibility, toxicity and impact pressure, etc.), factors of jet fire and high-temperature mixture (JFHM) (ejection height/ length, ejection temperature), and factors of thermal runaway ejected powder (powder particle size, powder toxicity, etc.). The surface temperature of the battery usually reflects the temperature change when thermal runaway occurs, and people may be burnt by the high temperature when approaching or touching. The trigger time of thermal runaway is usually the time from a certain time to the occurrence of thermal runaway. It reflects the reaction time left for the operator when the battery is in a certain heating state to deal with thermal runaway. The lower gas explosion limit reflects the risk of the combustible gas ejected from LIBs when thermal runaway occurs. If an ignition source is encountered, it may explode, causing further damage. The gas toxicity reflects the risk of toxic vented gases due to the complexity of the thermal runaway

* Corresponding author.
E-mail address: wangzhirong@njtech.edu.cn (Z. Wang).

https://doi.org/10.1016/j.est.2021.103767
Received 21 September 2021; Received in revised form 16 November 2021; Accepted 4 December 2021
Available online 17 December 2021

Nomenclature

LIB	lithium-ion battery
AHP	analytic hierarchy process
JFHM	jet fire and high-temperature mixture
FAHP	fuzzy analytic hierarchy process
LEL	lower explosion limit
UEL	upper explosion limit
NCM	$Li(Ni_xCo_yMn_z)O_2$
LFP	$LiFePO_4$
LCO	$LiCoO_2$
NCA	$Li(Ni_xCo_yAl_z)O_2$
THI	toxicant hazardous index
k_i	sub-index weight of toxicant hazardous index
F_i	sub-index integral value of toxicant hazardous index
$\widetilde{X}$	fuzzy pair-wise comparison matrix
$\sim x_{ij}$ ($\widetilde{x}$)	fuzzy number in a pair-wise comparison matrix
n	sequence number of the factor or sub-factor
a, m, d	crisp numbers involved in fuzzy numbers
N	defuzzified crisp value of a triangular fuzzy number
CR	consistency ratio
CI	consistency index
RI	random index
$\widetilde{Tri}_{s,i}$	sum of triangular fuzzy numbers of the *i*th row in a pair-wise comparison matrix
$\widetilde{Tri}_s$	sum of $\widetilde{Tri}_{s,i}$
$\widetilde{w}_{tri,i}$	triangular fuzzy weight of the *i*th factor or sub-factor
$\widetilde{W}_{tri}$	triangular fuzzy weight vector of factor A
$\sim W_{tri,B_i}$	triangular fuzzy weight vector of sub-factors under the factor Bi
$w_i^{'}$	crisp weight the *i*th factor or sub-factor calculated by the triangular fuzzy approach
$W^{'}$	crisp weight vector used by the triangular fuzzy approach
w	normalized crisp weight calculated by the triangular fuzzy approach
W_{tri}	normalized crisp weight vector of factor A used by the triangular fuzzy approach
W_{tri,B_i}	normalized crisp weight vector of sub-factors under the factor B*i* used by the triangular fuzzy approach
$\widetilde{f}_{tri,c_{ij}}$	triangular fuzzy evaluating number of the sub-factor C_{ij}
$\sim F_{tri,B_i}$	triangular fuzzy evaluating vector of sub-factors under the factor B*i*
$\widetilde{f}_{tri,B_i}$	triangular fuzzy evaluating number of the factor B_i
$\sim F_{tri}$	triangular fuzzy evaluating vector of factor A
$\sim Z_{tri}$	evaluated result of factor A using the triangular fuzzy approach

Greek symbols

ρ_∞	air density, kg·m^{-3}
α, β, γ	crisp numbers involved in triangular fuzzy numbers
λ_{max}	the largest eigenvalue of the defuzzified pair-wise comparison matrix

reactions. The gas impact pressure is caused by the large amount of gas emitted in a short period of time when an LIB has a thermal runaway. People in the surrounding environment may be hurt by this kind of impact pressure. The JFHM ejected from the thermal runaway of LIBs has a long injection distance and its temperature is very high. The thermal runaway ejected powder affects the possibility of dust explosion and occupational health. The smaller the particle size, the greater the risk of dust explosion, and the greater the impact on the respiratory system of people. The ejected powder toxicity is owing to the toxic ingredients due to the complexity of the ejected powder during thermal runaway reactions. In this paper, fuzzy analytic hierarchy process (FAHP) is used to establish a comprehensive multi-parameter evaluation system for the risk of LIBs thermal runaway. This method systematically and quantitatively evaluates the risk of thermal runaway of LIBs from the overall point of view, based on the risk of thermal runaway process and product consequences. Based on the experimental results and literature data, the method is verified by case study and analysis.

In Section 2, the research method adopted in this paper, FAHP, is introduced briefly. The Sections 3 and 4 establish a detailed multi-parameter evaluation system, including evaluation index system, and weight calculation. The thermal runaway process under selected abuse condition is chosen, and a case study is carried out by using the evaluation method In Section 5. The main conclusions of this work are summarized in Section 6.

2. Methodology

In this paper, the fuzzy AHP method is used to analyze the thermal runaway risk from LIBs with multiple factors. AHP is a decision analysis method developed by Saaty [8,9] for evaluation, selection, ranking and prediction. The AHP can quantify the decision-making process with less analysis, and conduct simple quantitative research on complex issues. However, the analysis process is vague due to human judgment during the comparison and judgment of AHP. Or, when consulting with experts, they often give some vague statements. Therefore, fuzzy numbers are usually introduced on the basis of AHP to improve this process, forming a fuzzy AHP (FAHP) [10]. FAHP has been widely used in risk assessment [11], risk management [12], risk assessment and analysis [13], etc. The AHP is a combination of qualitative and quantitative decision-making analysis methods to solve complex problems. It has been widely used in engineering planning, scheme sequencing, risk analysis and other fields [14–16].

Various FAHP models have been developed by researchers. This paper refers to the relatively widely used triangular fuzzy numbers AHP [17,18] to conduct multi-factor evaluation and analysis on the thermal runaway risk of LIBs. The main steps of AHP include the establishment of evaluation index system, the calculation of weight, and the division of evaluation grade [18,19]. Thermal runaway of LIB will cause a series of hazards such as high temperature, fire, explosion, shock wave and so on [20–24]. Therefore, the risk evaluation of thermal runaway should be carried out systematically as a whole, considering the influence of various dangerous factors, so as to make a better quantitative evaluation and analysis. AHP divides the analyzed problem into three levels: objectives, factors and sub-factors for overall analysis, which is very suitable for comprehensive analysis of thermal runaway risk of LIBs.

In the past research, researchers have developed a variety of fuzzy evaluation methods applicable to different evaluation objectives [17–19,25]. For the multi-factor risk assessment of LIBs in this study, the triangular extent fuzzy analysis method developed by Chang [17] is selected for research and analysis.

3. Multi-factor evaluation index system

On the basis of combining experimental results and literature data, this paper first establishes an evaluation index system (A). It contains four basic factors: own hazardous factor of battery (B_1), hazardous factor of vented gases (B_2), hazardous factor of JFHM (B_3) and hazardous factor of ejected powder (B_4). Each basic factor contains a set of sub-factors. Since the previous works [26–29] show no obvious correlation (dependence) between the various states of charge (SOCs) of the battery and the sub-factors. Meanwhile, this paper conducts a risk analysis. The sub-factors are the performance of the risk and are affected by the decompositions or chemical reactions of the internal materials in the battery. Therefore, there is basically no mutual influence between the sub factors. It can be seen that the basic factors and sub-factors all meet the requirements of mutual independence. The hierarchical evaluation index system for LIBs thermal runaway risk in this paper is shown in Fig. 1. The own hazardous factor of battery (B_1) is mainly concerned about its own dangerous state when the battery has a thermal runaway. The jet fire and high-temperature mixture (JFHM) contains flames, hot gases and solid particles. Their common feature is the high thermal damage caused by high temperatures. Therefore, the hazardous factor of JFHM (B_3) is determined in order to focus on the scope and extent of damage caused by high-temperature ejection. The hazardous characteristics of vented gases are explosion hazard, toxicity and pressure and are characterized by hazardous factor of vented gases (B_2). Similarly, hazardous factor of ejected powder (B_4) mainly studies the toxicity and flammability of solid particles.

3.1. Own hazardous factor of battery (B_1)

For the LIB with thermal runaway, its own changes are the most significant and intuitive. The dangerous factors of the battery itself can directly affect the equipment and personnel in contact with it, and the impact caused by it is relatively large. Two sub-factors related to the own hazardous factors of battery are considered: surface temperature (C_{11}) and thermal runaway trigger time (C_{12}).

Surface temperature (C_{11}): the surface temperature of the battery usually reflects the temperature change of the battery surface when it has thermal runaway, and personnel may be burnt by the high temperature when in contact with it. Fu et al. [30] conducted a combustion test on a 18650 LIB in a cone calorimeter, and a thermocouple was used to measure the change of the surface temperature of the battery during thermal runaway, and the highest temperature was recorded. Chen et al. [24] used a VSP2 instrument to measure the temperature change of the battery during thermal runaway through the temperature system of the instrument with different SOC 18650 batteries, and the highest temperatures of the battery under various conditions were summarized. Liu et al. conducted a study with a self-made heating copper tube and a matching thermocouple to measure the temperature change of a thermal runaway battery during different heating powers, different SOCs, different charging and discharging processes [31]. Chen et al. [26] measured the impact pressure of the thermal runaway process, the temperature change on the battery surface was also recorded at the same time, and the highest temperature value under each condition was summarized. Therefore, in this evaluation model, the highest surface temperature of the battery during thermal runaway is used as one of the own hazardous factors of battery. The higher the maximum temperature of the battery surface, the more violent the internal reaction of the battery, and the greater the danger.

Thermal runaway trigger time (C_{12}): the thermal runaway trigger time is usually from a certain time to the time when thermal runaway occurs. It reflects the reaction time left for the operator to deal with the thermal runaway when the battery is in a certain heating state. Ouyang et al. [32] conducted a thermal runaway heating test on an LIB pack in a cone calorimeter. The heating power of 2.0 kW is used to heat the battery packs of different SOCs with electric heating system. The relevant data such as safety valve opening time, fire time, thermal runaway time are recorded. In the battery combustion test of Fu et al. [30], the fire time and thermal runaway explosion time under different heating conditions were also counted and recorded. Chen et al. [26] measured the impact pressure from the thermal runaway, and also recorded the interval time from the battery safety valve opening to the intense ejection stage of thermal runaway during the heating process ($t_{SVO\text{-}IES}$). In general, the temperature rise mainly depends on the power of the external heating device before opening of the battery safety valve. After the valve is opened, the internal reaction heat exceeds the heat dissipation of the battery when the temperature rises to a certain temperature, and the battery enters a self-accelerating heating state. Therefore, in this evaluation model, the interval time from the opening of battery safety valve to the intense ejection stage of thermal runaway is defined as the thermal runaway trigger time. And it is also used as one of the own hazardous factors of battery. The shorter the thermal runaway trigger time, the harsher the abuse environment the surface battery is in, and its risk is higher.

3.2. Hazardous factor of vented gases (B_2)

The vented gas from LIBs thermal runaway is dangerous, fluid, and has a high degree of concern. Three sub-factors related to the hazardous

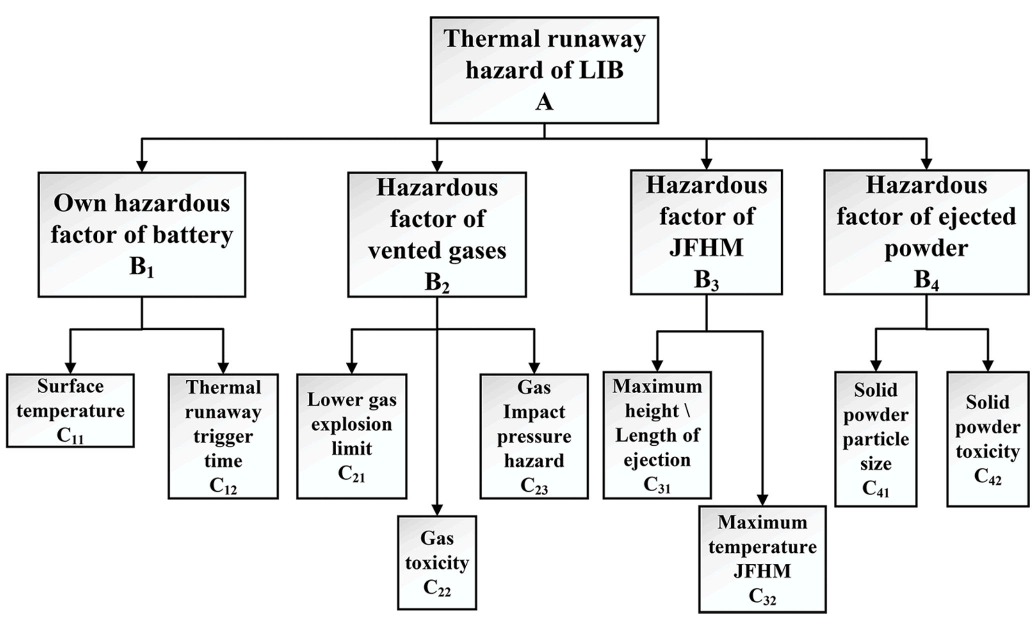

Fig. 1. The hierarchy index system for multi-parameter evaluation on thermal runaway of LIB.

factors of vented gases are considered: lower gas explosion limit (C_{21}), gas toxicity (C_{22}) and gas impact pressure hazard (C_{23}).

Lower gas explosion limit (C_{21}): when thermal runaway occurs, products containing combustible gas will be ejected from LIBs. The gases may explode if it encounters an ignition source, causing further damage. Baird et al. [33] summarized and compared the experimental test results and theoretical calculation prediction results of the lower explosion limit (LEL) of thermal runaway gas of four cathode materials (NCM, LFP, LCO, NCA) conducted by former studies. Li et al. [34] used the composition data of the thermal runaway vented gas from literature, to calculate and analyze the LEL, the upper explosion limit (UEL) and the explosion range of the thermal runaway gas combined with theoretical formulas. Because the amount of thermal runaway vented gas is relatively limited, and it contains a certain amount of inert gas in addition to the combustible gas. It is more likely that the concentration of combustible gas will change near the LEL, but it is relatively difficult to reach the UEL. With the LEL data, it can basically be judged whether the vented gas by thermal runaway meets the explosion conditions. Therefore, in this evaluation model, the LEL is used as one of the hazardous factors of vented gases. The lower the LEL is, the easier it is to reach the explosion condition, and the higher the explosion risk.

Gas toxicity (C_{22}): due to the complexity of the thermal runaway reactions of LIBs, some of the vented gases may be toxic, in addition to the combustion and explosion. Hammami et al. [35] studied the mechanism and toxicity of toxic fluorides that may be generated from the reactions between the electrolyte and the positive electrode material with LIBs under abuse conditions. Larsson et al. [36] measured the changes in hydrogen fluoride and phosphorus oxyfluoride released by seven different brands and models of LIBs thermal runaway. Except for the toxic fluorides, LIBs will release carbon monoxide and a variety of toxic organic compounds during thermal runaway, such as 2-propenal, propanedinitrile, carbonyl sulfide, and sulfur dioxide etc [37]. To quantitatively evaluate the gas toxicity released by thermal runaway, the calculation method of the toxicant hazardous index (*THI*) from the Chinese National Occupational Health Standard "Classification for hazards of occupational exposure to toxicant" GBZ 230–2010 [38] was referred. This calculation method can be used to calculate the toxicity of substances, the *THI* can be calculated as Eq. (1):

$$THI = \sum_{i=1}^{n} (k_i \cdot F_i) \tag{1}$$

where k_i is the sub-index weight of toxicant hazardous index, F_i is the sub-index integral value of toxicant hazardous index. The relevant sub-index weights and integral values are calculated according to the classification and scoring standards of occupational exposure to toxicant hazards given by the standard. Since the gas produced by thermal runaway is a mixture, the F_i of the most harmful substance in the mixture is selected as the F_i of the mixture in each item. Finally, the degree of harm is divided into five levels according to the calculation results. The risk grades of the factors in this evaluation model refers to this standard and corresponds to these five levels.

Gas impact pressure hazard (C_{23}): When an LIB has a thermal runaway, the large amount of gas emitted in a short period of time will cause the pressure of the surrounding environment to rise rapidly. If a person is nearby, he or she may be injured by this impact pressure. According to the research conducted by Chen et al. [26], the damage of impact pressure has a numerical relationship with the value and duration of the pressure. Therefore, in this evaluation model, according to the value (ordinate) and duration (abscissa) of the impact pressure generated by thermal runaway, the position of the point on the Bowen curves is drawn to determine the risk of impact pressure. Falling into different levels of danger zones means different levels of danger.

3.3. Hazardous factor of JFHM (B_3)

The JFHM ejected from the thermal runaway of LIBs has a long injection distance and its temperature is very high. Two sub-factors related to the hazardous factors of JFHM are considered: maximum height/ length of ejection (C_{31}) and maximum temperature of JFHM (C_{32}).

Maximum height/ length of ejection (C_{31}): Chen et al. [28] revealed that the JFHM will cause injury to surrounding personnel or equipment. In order to eliminate the difference in shape and size between different types of batteries, in this evaluation model, the dimensionless maximum height (vertical placement)/ length (horizontal placement) of the JFHM ejected from thermal runaway is used as one of the hazardous factors of JFHM. The higher the dimensionless height or the longer the dimensionless length of the JFHM, the greater is the risk.

Maximum temperature of JFHM (C_{32}): Chen et al. [28] also indicated that the reason why the ejection of the JFHM will cause damage to the surrounding personnel or equipment is that the ejected product has a very high temperature. Therefore, in this evaluation model, the maximum temperature of the JFHM during thermal runaway is used as one of the hazardous factors of JFHM. The higher the temperature of the JFHM, the greater is the danger.

3.4. Hazardous factor of ejected powder (B_4)

The ejected solid powder produced by thermal runaway of LIBs has a certain degree of danger. Two sub-factors related to the hazardous factor of ejected powder: ejected powder particle size (C_{41}) and ejected powder toxicity (C_{42}).

Ejected powder particle size (C_{41}): Chen et al. [29] analyzed the ejected powder and found out that, except for the influence of solid powder particle size on the possibility of dust explosion, the smaller the particle size, the greater the impact is on the respiratory system of personnel. Therefore, according to these research results, the ejected powder particle size is used as one of the hazardous factors of ejected powder. The smaller the particle size, the greater is the risk.

Ejected powder toxicity (C_{42}): according to the test results conducted by Chen et al. [29], due to the complexity of the ejected powder from thermal runaway, it contains a certain amount of toxic ingredients. There may be a poisoning hazard if personnel contact it by mistake. Therefore, the Chinese National Occupational Health Standard "Classification for hazards of occupational exposure to toxicant" GBZ 230–2010 [38] was also referred to do the *THI* calculation of the hazardous substances in the ejected powder, which was the same as the evaluation on gas toxicity (C_{22}).

4. Calculation of weight

In FAHP, linguistic variables are usually used to describe the relative importance of factors. In order to calculate, linguistic variables need to be converted into corresponding fuzzy scales. The triangular fuzzy scales of relative importance are used in this FAHP and shown in Table 1 [17, 18].

4.1. Establishment of pair-wise comparison matrix

The pair-wise comparison matrix used in this FAHP can be expressed

Table 1
Triangular fuzzy numbers of relative importance.

Linguistic variable	Triangular fuzzy number
Equally important (preponderant)	(1, 1, 1)
Weakly important (preponderant)	(1, 3/2, 2)
Essentially important (preponderant)	(3/2, 2, 5/2)
Very strongly important (preponderant)	(2, 5/2, 3)
Absolutely important (preponderant)	(5/2, 3, 7/2)

Table 2
Fuzzy numbers for LIB thermal runaway risk (factor A).

	B_1	B_2	B_3	B_4
B_1	(1, 1, 1)	(2/5, 1/2, 2/3)	(2/5, 1/2, 2/3)	(1/2, 2/3, 1)
B_2	(3/2, 2, 5/2)	(1, 1, 1)	(1, 3/2, 2)	(1, 3/2, 2)
B_3	(3/2, 2, 5/2)	(1/2, 2/3, 1)	(1, 1, 1)	(1, 3/2, 2)
B_4	(1, 3/2, 2)	(1/2, 2/3, 1)	(1/2, 2/3, 1)	(1, 1, 1)

Table 3–1
Fuzzy numbers for the battery itself (factor B_1).

	C_{11}	C_{12}
C_{11}	(1, 1, 1)	(1/2, 2/3, 1)
C_{12}	(1, 3/2, 2)	(1, 1, 1)

Table 3–2
Fuzzy numbers for the risk of the vented gas (factor B_2).

	C_{21}	C_{22}	C_{23}
C_{21}	(1, 1, 1)	(3/2, 2, 5/2)	(1, 3/2, 2)
C_{22}	(2/5, 1/2, 2/3)	(1, 1, 1)	(1/2, 2/3, 1)
C_{23}	(1/2, 2/3, 1)	(1, 3/2, 2)	(1, 1, 1)

Table 3–3
Fuzzy numbers for the risk of the JFHM (factor B_3).

	C_{31}	C_{32}
C_{31}	(1, 1, 1)	(1, 3/2, 2)
C_{32}	(1/2, 2/3, 1)	(1, 1, 1)

Table 3–4
Fuzzy numbers for the risk of the ejected powder (factor B_4).

	C_{41}	C_{42}
C_{41}	(1, 1, 1)	(1, 3/2, 2)
C_{42}	(1/2, 2/3, 1)	(1, 1, 1)

Table 4
The random consistency index (*RI*).

	1	2	3	4	5	6	7	8	9
RI	0	0	0.58	0.90	1.12	1.24	1.32	1.41	1.45

as [18]:

$$\widetilde{X} = (x_{ij})(i, j = 1, 2, \cdots, n) \tag{2}$$

$$\sim x_{ij} = (a_{ij}, m_{ij}, d_{ij}) \tag{3}$$

$$\sim x_{ji} = (\sim x_{ij})^{-1} = (d_{ij}{}^{-1}, m_{ij}, a_{ij}{}^{-1}) \tag{4}$$

where $\sim X$ is the pair-wise comparison matrix, $\sim x_{ij}$ is the elements in the pair-wise comparison matrix, n is the number of the factor or sub-factors. Therefore, the pair-wise comparison matrix of factor and sub-factors are established based on the analysis above, and are shown in Tables 2 and 3.

4.2. Consistency check

After being established, the consistencies of the matrices need to be checked to ensure that the defined weights of the matrices are acceptable. Firstly, according to Eq. (5), the fuzzy numbers in the fuzzy matrices in Tables 2 and 3 need to be converted into matching crisp values [18].

$$N = \frac{m + m}{2} + \frac{[(d - m) - (m - a)]}{6} = \frac{a + 4m + d}{6} \tag{5}$$

Then the largest eigenvalue ($\lambda_{\max}$) of the defuzzified matrix can be calculated. Lastly, the consistency of the matrix is calculated by the consistency ratio (CR).

$$CR = CI/RI \tag{6}$$

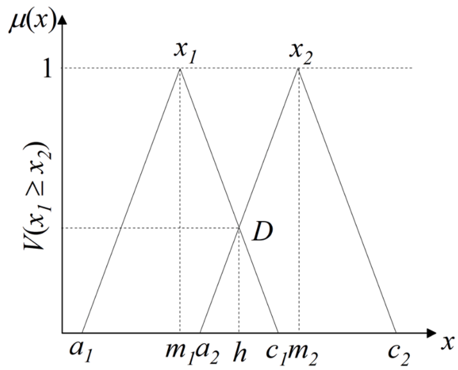

Fig. 2. The intersection between two triangular fuzzy numbers $\widetilde{x}_1$ and $\widetilde{x}_2$.

$$CI = (\lambda_{max} - n)/(n-1) \tag{7}$$

where *CI* is the consistency index, *RI* is the random index, as shown in Table 4 [18]. When the CR < 0.1, the consistency of the matrix can be considered acceptable. Otherwise, the pair-wise comparison matrix should be modified to meet the requirements of consistency.

4.3. Weight calculation of factors

4.3.1. Fuzzy weight vectors by triangular method

The calculation of the triangular fuzzy weights includes two steps [18]. First, the triangular fuzzy weights are calculated by the general method, and then the crisp weight is calculated by the triangular extent analysis. The sum of the triangular fuzzy numbers in the *i*th row of the pair-wise comparison matrix is shown in Eq. (8):

$$\sim Tri_{s,i} = \sum_{j=1}^{n} \widetilde{x}_{ij} = \left(\alpha_{tri,i}, \beta_{tri,i}, \gamma_{tri,i}\right) \tag{8}$$

The sum of $\sim Tri_{s,i}$ is shown in Eq. (9):

$$\sim Tri_{s} = \sum_{i=1}^{n} \widetilde{Tri}_{s,i} = \left(\alpha_{tri}, \beta_{tri}, \gamma_{tri}\right) \tag{9}$$

So, the triangular fuzzy weight of the *i*th factor or sub-factor is defined as:

$$\widetilde{w}_{tri,i} = \widetilde{Tri}_{s,i}\,(\phi)\widetilde{Tri}_{s} = \left(\alpha_{tri,i}{\gamma_{tri}}^{-1}, \beta_{tri,i}{\beta_{tri}}^{-1}, \gamma_{tri,i}{\alpha_{tri}}^{-1}\right) \tag{10}$$

Therefore, the triangular fuzzy weight vectors of factor A ($\widetilde{W}_{tri}$) and sub-factors B$_i$ ($\widetilde{W}_{tri,B_i}$) can be written as:

$$\widetilde{W}_{tri} = \left(\widetilde{w}_{tri,B_1}, \widetilde{w}_{tri,B_2}, \widetilde{w}_{tri,B_3}\right) \tag{11}$$

$$\widetilde{W}_{tri,B_i} = \left(\widetilde{w}_{tri,c_{i1}}, \widetilde{w}_{tri,c_{i2}}, \dots, \widetilde{w}_{tri,c_{ik}}\right) \tag{12}$$

4.3.2. Normalized crisp weight vectors of factors

Based on the triangular fuzzy weight vectors defined above, the weights can be optimized to obtain more accurate values using the characteristics of the triangular fuzzy number and comparing with other elemental weights. In view of this, it is necessary to perform a triangular extent analysis on the above triangular fuzzy weights [18]. The degree of possibility of $\widetilde{x}_1 = (a_1, m_1, d_1) \geq \widetilde{x}_2 = (a_2, m_2, d_2)$ is defined as follows:

$$V(\widetilde{x}_1 \geq \widetilde{x}_2) = \mu_{\widetilde{x}_1}(h) = \begin{cases} 1, & \text{if } m_1 \geq m_2 \\ 0, & \text{if } a_2 \geq d_1 \\ \dfrac{a_2 - d_1}{(m_1 - d_1) - (m_2 - a_2)} & \text{otherwise} \end{cases} \tag{13}$$

where *h* is the abscissa of the highest intersection point *D* between $\mu_{\widetilde{x}_1}$ and $\mu_{\widetilde{x}_2}$, as shown in Fig. 2 [18].

Table 5
The consistency check results and calculated weights.

Factor	Fuzzy weight vector, $\widetilde{W}$	Extent analysis weights, *w*	Largest eigenvalue, λ_{max}	Consistency ratio
B$_1$	(0.103, 0.151, 0.242)	0.068	4.072	Consistent (CR=0.027)
B$_2$	(0.201, 0.340, 0.543)	0.386		
B$_3$	(0.179, 0.292, 0.471)	0.328		
B$_4$	(0.134, 0.217, 0.362)	0.219		
C$_{11}$	(0.300, 0.400, 0.571)	0.316	2.021	Consistent (No need for CR calculating)
C$_{12}$	(0.400, 0.600, 0.857)	0.684		
C$_{21}$	(0.288, 0.458, 0.696)	0.558	3.036	Consistent (CR=0.031)
C$_{22}$	(0.156, 0.220, 0.338)	0.097		
C$_{23}$	(0.205, 0.322, 0.506)	0.345		
C$_{31}$	(0.400, 0.600, 0.857)	0.684	2.021	Consistent (No need for CR calculating)
C$_{32}$	(0.300, 0.400, 0.571)	0.316		
C$_{41}$	(0.400, 0.600, 0.857)	0.684	2.021	Consistent (No need for CR calculating)
C$_{42}$	(0.300, 0.400, 0.571)	0.316		

Table 6
Linguistic variables and their fuzzy numbers for five criteria risk grades.

Linguistic variables	Triangular fuzzy numbers
Very dangerous (VD)	(7, 17/2, 10)
Dangerous (D)	(5, 13/2, 8)
Medium (M)	(3, 9/2, 6)
Safe (S)	(1, 5/2, 4)
Very safe (VS)	(0, 3/2, 3)

To compare the value of $\widetilde{x}_1$ and $\widetilde{x}_2$, the values of $V(\widetilde{x}_1 \geq \widetilde{x}_2)$ and $V(\widetilde{x}_2 \geq \widetilde{x}_1)$ are needed. The degree of possibility for a convex fuzzy number to be greater than *p* convex fuzzy numbers $\widetilde{x}_i (i = 1, 2, \dots, p)$ is expressed as:

$$V\left(\widetilde{x} \geq \widetilde{x}_1, \widetilde{x}_2, \dots, \widetilde{x}_p\right) = V\left[\left(\widetilde{x} \geq \widetilde{x}_1\right) \text{and} \left(\widetilde{x} \geq \widetilde{x}_2\right) \dots \text{and} \left(\widetilde{x} \geq \widetilde{x}_p\right)\right] = \min\left(V\left(\widetilde{x} \geq \widetilde{x}_i\right)\right) \tag{14}$$

Therefore, according to the above triangular extent fuzzy analysis, the crisp weight of the *i*th factor or sub-factor is shown in Eq. (15):

$$w_i^{'} = \min\left(V\left(\widetilde{w}_{tri,i} \geq \widetilde{w}_{tri,p}\right)\right) \quad p = 1, 2, \cdots, n, p \neq i \tag{15}$$

where $w_i^{'}$ is the crisp weight of the *i*th factor or sub-factor, and it is a non-fuzzy number. So the crisp weight vector is defined as:

$$W^{'} = \left(w_1^{'}, w_2^{'}, \dots, w_n^{'}\right) \tag{16}$$

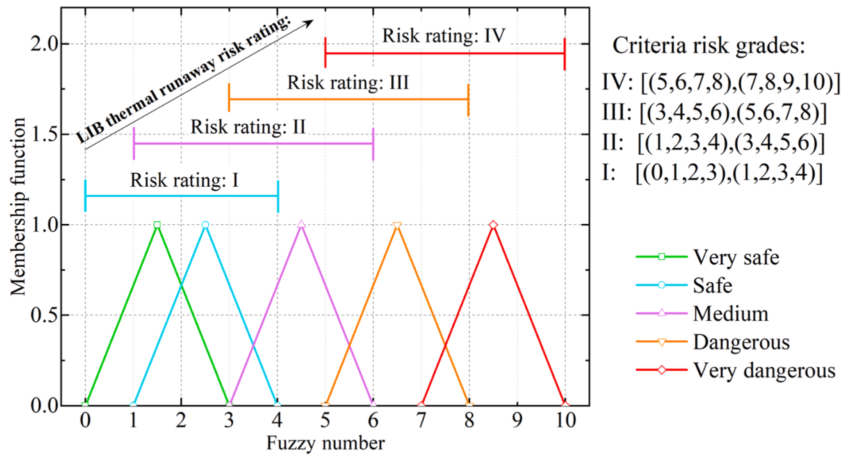

Fig. 3. The criteria risk grades of factors and sub-factors and the criteria risk ratings of LIB thermal runaway.

Table 7
The criteria risk grades and their parameters' ranges.

Sub-factors	Risk grades				
	VS	S	M	D	VD
Surface temperature, C_{11} (°C) [24,27,30]	<70	[70, 200]	[200, 410]	[410, 750]	>750
Thermal runaway trigger time, C_{12} (s) [26,29]	>300	[180, 300]	[60, 180]	[30, 60]	<30
Lower gas explosion limit, C_{21} (%) [33,34]	>45	[21, 45]	[9, 21]	[5, 9]	<5
Gas toxicity (*THI*), C_{22} [38]	<1	[1, 35]	[35, 50]	[50, 65]	>65
Gas impact pressure hazard, C_{23} [26]	$<LD_1$	$[LD_1, LD_{10}]$	$[LD_{10}, LD_{50}]$	$[LD_{50}, LD_{90}]$	$>LD_{90}$
Maximum height/ length of ejection, C_{31} [28]	<0.5	[0.5, 1]	[1, 3]	[3, 5]	>5
Maximum temperature of JFHM, C_{32} (°C) [28]	<70	[70, 350]	[350, 600]	[600, 700]	>700
Ejected powder particle size, C_{41} (μm) [29]	>100	[50, 100]	[20, 50]	[15, 20]	<15
Ejected powder toxicity (*THI*), C_{42} [38]	<1	[1, 35]	[35, 50]	[50, 65]	>65

The normalized crisp weight vectors of factor A (W_{tri}) and sub-factors B*i* (W_{tri,B_i}) can be expressed as Eqs. (17) and (18) by normalization:

$$W_{tri} = \left(w_{tri,B_1}, w_{tri,B_2}, w_{tri,B_3}\right) \tag{17}$$

$$W_{tri,B_i} = \left(w_{tri,c_{i1}}, w_{tri,c_{i2}}, \dots, w_{tri,c_{ik}}\right) \tag{18}$$

4.3.3. Results of weight calculation

According to the above calculation method of fuzzy weight and crisp weight, for the defined multi-factor evaluation index system, the consistency check results and calculated weights of the pair-wise comparison matrices of the multi-factor evaluation for the risk of LIBs thermal runaway are shown in Table 5.

5. Case study

In this study, the fuzzy evaluation method was used to evaluate the risk of LIBs thermal runaway. First of all, the risk grades must be determined, and then the risk rating process will be carried out.

5.1. Determination of risk grades

In the determination of risk grades, the transformation from the linguistic variables to the fuzzy evaluating numbers is established., and then the risk ratings can be obtained.

Table 8
The risk ratings of LIB thermal runaway.

Risk rating	Description	Evaluated result using the triangular fuzzy approach
IV	The LIB is very dangerous after thermal runaway	$(5, 13/2, 8) \le \sim Z_{tri} \le (7, 17/2, 10)$
III	The LIB is more dangerous after thermal runaway	$(3, 9/2, 6) \le \sim Z_{tri} \le (5, 13/2, 8)$
II	The LIB is dangerous after thermal runaway	$(1, 5/2, 4) \le \sim Z_{tri} \le (3, 9/2, 6)$
I	The LIB is safe after thermal runaway	$(0, 3/2, 3) \le \sim Z_{tri} \le (1, 5/2, 4)$

5.1.1. Risk grades of five criteria

The risk grades are divided into five levels: very dangerous (VD), dangerous (D), medium (M), safe (S) and very safe (VS). The corresponding rules for converting of linguistic variables into triangular fuzzy numbers are shown in the Table 6 and Fig. 3 [18].

According to the previous analysis, Table 7 lists the five criteria risk grades of the 9 sub-factors and their ranges.

Table 9
Statistics of thermal runaway risk parameters from LIB and fuzzy evaluating numbers.

Parameter	Data	Risk grade	Triangular fuzzy numbers
Surface temperature, C_{11} (°C)	676.5 [26]	D	(5, 13/2, 8)
Thermal runaway trigger time, C_{12} (s)	272.9 [26]	S	(1, 5/2, 4)
Lower gas explosion limit, C_{21} (%)	5.08 [27]	D	(5, 13/2, 8)
Gas toxicity (*THI*), C_{22} [a]	77	VD	(7, 17/2, 10)
Gas impact pressure hazard, C_{23}	$[LD_1, LD_{10}]$ [28]	S	(1, 5/2, 4)
Maximum height/ length of ejection, C_{31}	4.41 [28]	D	(5, 13/2, 8)
Maximum temperature of JFHM, C_{32} (°C)	566.4 [28]	M	(3, 9/2, 6)
Ejected powder particle size, C_{41} (μm)	188.82 [29]	VS	(0, 3/2, 3)
Ejected powder toxicity (*THI*), C_{42} [b]	49	M	(3, 9/2, 6)

a: gas composition data is from Ref. [27]. The sub-index integral value of the most harmful substance in the mixture is selected as the sub-index integral value of the gas mixture in each item, as shown in Table 10–1.
b: ejected powder composition data is from Ref. [29]. The sub-index integral value of the most harmful substance in the mixture is selected as the sub-index integral value of the solid mixture in each item, as shown in Table 10–2.

5.1.2. Calculation of risk ratings

The collected data of the sub-factors are compared with the parameters' ranges in Table 7 to determine different risk grades. Then the fuzzy numbers can be obtained via risk grades from Table 6. Therefore, the triangular fuzzy evaluating vector of sub-factor B_i is shown as Eq. (19):

$$\widetilde{F}_{tri,B_i} = \left(\widetilde{f}_{tri,c_{i1}}, \ldots, \widetilde{f}_{tri,c_{ij}}, \ldots, \widetilde{f}_{tri,c_{ik}}\right) \tag{19}$$

where $\widetilde{f}_{tri,c_{ij}}$ is the triangular fuzzy evaluating number of the sub-factor C_{ij}. Therefore, the triangular fuzzy evaluating number of the sub-factor B_i can be obtained by the product of the normalized crisp weight and the triangular fuzzy evaluation number of the sub-factors, as shown in Eq. (20):

$$\widetilde{f}_{tri,B_i} = \sum_{j=1}^{k}\left(w_{tri,c_{ij}} (\otimes) \widetilde{f}_{tri,c_{ij}}\right) \tag{20}$$

where, $\widetilde{f}_{tri,B_i}$ is the triangular fuzzy evaluating number of the sub-factor B_i, $w_{tri,c_{ij}}$ is the normalized crisp weight of the sub-factor C_{ij}. Therefore, the triangular fuzzy evaluating vector of factor A can be calculated by Eq. (21):

$$\widetilde{F}_{tri} = \left(\widetilde{f}_{tri,B_1}, \widetilde{f}_{tri,B_2}, \widetilde{f}_{tri,B_3}\right) \tag{21}$$

Lastly, the evaluated result of factor A using the triangular fuzzy approach can be calculated according to the normalized crisp weight and the triangular fuzzy evaluation number of the sub-factor B_i, as shown in Eq. (22):

$$\widetilde{Z}_{tri} = \sum_{i=1}^{n}\left(w_{tri,B_i} (\otimes) \widetilde{f}_{tri,Bi}\right) \tag{22}$$

The risk rating can be obtained by comparing the evaluated result of factor A with Fig. 3 or Table 8 [18].

5.2. The multi-parameter evaluated risk ratings

To test the effectiveness of the evaluation method and conduct a targeted case analysis, a process of LIB thermal runaway that occurred in a more dangerous abuse condition was selected for risk analysis. The selected abuse condition refers to placing a 100% SOC battery vertically, heating it to have a thermal runaway in the air with a heating power of 400 W and a heating temperature of 300 °C. The battery type is Samsung ICR18650-26J M 18650, with a diameter of 18 mm and a height of 65 mm and is cylindrical. The battery consists of intercalated graphite anode, lithiated metal oxide cathode (cobalt, nickel and manganese) and an electrolyte composed of ethylene carbonate, propylene carbonate, diethyl carbonate and lithium hexafluorophosphate. The material of the separator is a two-layer structure made from polyethylene (PE). The data measured in our previous work or in the public literature were used as the risk parameter.

The thermal runaway risk parameters and data at the selected abuse condition is summarized in Table 9, with the corresponding risk grades and triangular fuzzy numbers by referencing Tables 6 and 7. All the batteries experiments conducted in Table 9 are the same types (Samsung ICR18650-26J M).

The triangular fuzzy evaluation number of the sub-factor B_i can be calculated by Eq. (20) with the triangular fuzzy numbers in Table 9 and extent analysis weights in Table 5. The evaluated risk grades can be obtained from Table 6.

Table 10–1
The toxicant hazardous index of the vented gas from LIB thermal runaway.

Integral index		Property	F	k
Acute inhalation LC_{50}	Gas (cm^3/m^3)	2104.66 (Rats) (Carbon monoxide)	2	5
	Vapour (mg/m^3)	–	–	
	Dust and smoke (mg/m^3)	–	–	
Acute oral LD_{50} (mg/kg)		–	–	–
Acute dermal LD_{50} (mg/kg)		48 (Mice) (Benzene)	4	1
Irritation and corrosion		Strong irritation (Benzene)	3	2
Sensitization		No sensitization	0	2
Reproductive toxicity		Reproductive toxicity of animals (Benzene)	3	3
Carcinogenicity		Type 1 carcinogen (Benzene)	4	4
Actual harmful consequence and prognosis		Severe occupational mortality ≥ 10% (Benzene)	4	5
Diffusivity (Room temperature or state of industrial use)		Gaseous state	4	3
Accumulation (or Biological half-life)		No accumulation	0	1
Toxicant hazardous index		$THI = \sum_{i=1}^{n}(k_i \cdot F_i)$=77		

Table 10–2
The toxicant hazardous index of the ejected powder from LIB thermal runaway.

Integral index		Property	F	k
Acute inhalation LC_{50}	Gas (cm^3/m^3)	–	–	–
	Vapour (mg/m^3)	–	–	
	Dust and smoke (mg/m^3)	–	–	
Acute oral LD_{50} (mg/kg)		525 (Rats) (Lithium carbonate)	3	5
Acute dermal LD_{50} (mg/kg)		–	–	–
Irritation and corrosion		Moderate irritation (Lithium carbonate)	2	2
Sensitization		Skin sensitivity (Nickel)	3	2
Reproductive toxicity		Reproductive toxicity of animals (Lithium salt)	2	3
Carcinogenicity		Type 2B carcinogen (Nickel, cobalt)	2	4
Actual harmful consequence and prognosis		Physical lesions (Powdered carbon)	2	5
Diffusivity (Room temperature or state of industrial use)		Solid-state, low diffusivity	0	3
Accumulation (or Biological half-life)		No accumulation	0	1
Toxicant hazardous index		$THI = \sum_{i=1}^{n}(k_i \cdot F_i)$=49		

Table 11
The fuzzy evaluating numbers of B_i and evaluated risk grades.

Factor	Triangular fuzzy number	Risk grade
B_1	(2.3, 3.8, 5.3)	<S, M>
B_2	(3.8, 5.3, 6.8)	<M, D>
B_3	(4.4, 5.9, 7.4)	<M, D>
B_4	(0.9, 2.4, 3.9)	<VS, S>

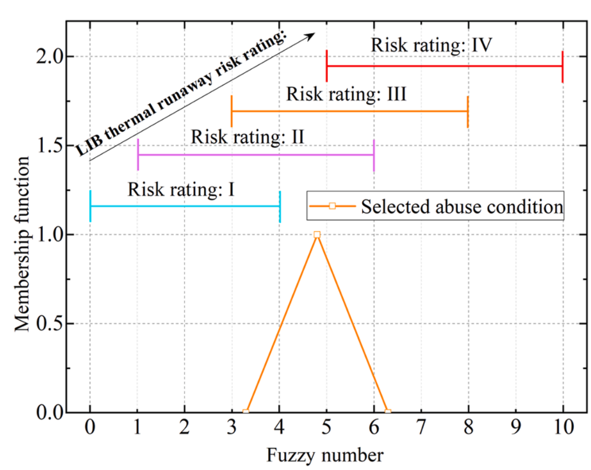

Fig. 4. The multi-parameter evaluated risk ratings on thermal runaway of LIB using the triangular fuzzy AHP approach.

The triangular fuzzy evaluated result of factor A can be calculated by Eq. (22) with the triangular fuzzy numbers in Table 11 and extent analysis weights of sub-factors B_i in Table 5:

$$\sim Z_{tri} = (3.3, 4.8, 6.3) \tag{23}$$

Therefore, according to Table 8 and Fig. 4, the calculated result is $(3, 9/2, 6) \leq \sim Z_{tri} = (3.3, 4.8, 6.3) \leq (5, 13/2, 8)$. The risk rating when the LIB conducts a thermal runaway at the selected abuse condition is III: the LIB is more dangerous after thermal runaway.

It can be further discussed that, from the results of this study, the priority (weight) of the sub-factors determined by the evaluation method can be used to determine the risk factors of key protection points. For example, according to Table 5, the hazards of gases and JFHM are relatively high among the thermal runaway risks of LIBs. The lower gas explosion limit and the maximum height/ length of ejection are the two sub-factors with the relatively greatest weights. Therefore, in engineering applications, the protection of the risk of thermal runaway from LIBs should focus on the possible explosion of thermal runaway gases, and the damage to surrounding personnel and equipment caused by thermal runaway jet fire and high-temperature mixtures.

6. . Conclusion

The LIB with thermal runaway under the selected abuse condition is chosen for risk analysis, so as to test the effectiveness of the evaluation method. The risk assessment scope of each factor is determined, and the corresponding calculation and analysis are carried out. The abuse condition selected is a more severe one. The thermal runaway generally has a more serious consequence on this condition, and the risk rating is III according to the evaluation method in this study. Therefore, the thermal runaway risk of LIBs analyzed according to this multi-factor evaluation method is more consistent with the actual risk, indicating that the evaluation system is relatively effective.

Compared with the previous risk evaluation methods of LIBs, the innovations of the multi-factors evaluation methods proposed are as follows:

(1) The thermal runaway risk can be comprehensively, systematically and integrally evaluated.
(2) It is guided by the consequences of thermal runaway. It obtains parameter data through experiments and combines the experimental data with theoretical methods to determine the risk. It is universal and dynamic. An evaluation system can be established to evaluate the risk of LIBs of any type, brand, and state to form a modified evaluation system to determine the risk rating.
(3) The risk factors of key protection can be determined according to the priority (weight) of the sub-factors analyzed by the evaluation.

In the follow-up research, a database of risk factors of thermal runaway from LIBs can be established according to actual needs, and corresponding evaluation software can be developed to improve the efficiency of fuzzy number calculation. Meanwhile, a complete set of test equipment systems with high degree of automation may be developed to obtain the experimental data of relevant parameters conveniently and quickly.

The mechanism, hazards, prevention and control of thermal runaway is still a challenging research topic. The factors and weights used in the evaluation method should also be optimized according to the continuous in-depth research, to obtain a more accurate and reasonable risk rating. The evaluation results get in this paper can provide reasonable guidance for the judgment and classification of the risk of thermal runaway at the present.

CRediT authorship contribution statement

Zhirong Wang: Resources, Supervision, Funding acquisition, Writing – original draft. **Shichen Chen:** Conceptualization, Investigation, Writing – original draft, Visualization. **Xinrui He:** Investigation, Writing – review & editing. **Chao Wang:** Investigation, Writing – review & editing. **Dan Zhao:** Investigation, Writing – review & editing.

Declaration of Competing Interest

The authors declare that they have no known competing financial interests or personal relationships that could have appeared to influence the work reported in this paper.

Acknowledgments

This work was supported by the National Natural Science Foundation of China [Grant No. 51874184], the Key R & D programs (Social Development) in Jiangsu Province [Grant No. BE2016771], the Key Natural Science Foundation in Jiangsu Province [Grant No. 18KJA620003], the Jiangsu Project Plan for Outstanding Talents Team in Six Research Fields [Grant No. TD-XNYQC-002], and the Postgraduate Research & Practice Innovation Program of Jiangsu Province [Grant No. KYCX20_1039]. Part of the work was funded by the National Natural Science Foundation of China [Grant No. U20A20213], and the Department of Science and Technology of Sichuan Province [Grant No. 2021JDTD0030].

References

[1] Z. Liao, S. Zhang, K. Li, M. Zhao, Z. Qiu, D. Han, G. Zhang, T.G. Habetler, Hazard analysis of thermally abused lithium-ion batteries at different state of charges, J. Energy Storage 27 (2020), 101065, https://doi.org/10.1016/j.est.2019.101065.
[2] J. Wang, W. Cai, X. Mu, L. Han, N. Wu, C. Liao, Y. Kan, Y. Hu, Construction of multifunctional and flame retardant separator towards stable lithium-sulfur batteries with high safety, Chem. Eng. J. 416 (2021), 129087, https://doi.org/10.1016/j.cej.2021.129087.
[3] P.J. Bugryniec, J.N. Davidson, D.J. Cumming, S.F. Brown, Pursuing safer batteries: thermal abuse of $LiFePO_4$ cells, J. Power Sources 414 (2019) 557–568, https://doi.org/10.1016/j.jpowsour.2019.01.013.
[4] Q. Wang, B. Mao, S.I. Stoliarov, J. Sun, A review of lithium ion battery failure mechanisms and fire prevention strategies, Prog. Energy Combust. Sci. 73 (2019) 95–131, https://doi.org/10.1016/j.pecs.2019.03.002.
[5] C.N. Ashtiani, Battery hazard modes and risk mitigation analysis, USABC, United States Advanced Battery Consortium, International Symposium on Large Lithium Ion Battery Technology and Application (2007).
[6] F.J. Soares, L. Carvalho, I.C. Costa, J.P. Iria, J.M. Bodet, G. Jacinto, A. Lecocq, J. Roessner, B. Caillard, O. Salvi, The STABALID project: risk analysis of stationary Li-ion batteries for power system applications, Reliab. Eng. Syst. Saf. 140 (2015) 142–175, https://doi.org/10.1016/j.ress.2015.04.004.
[7] F.H. Gandoman, J. Jaguemont, S. Goutam, R. Gopalakrishnan, Y. Firouz, T. Kalogiannis, N. Omar, J. van Mierlo, Concept of reliability and safety assessment of lithium-ion batteries in electric vehicles: basics, progress, and challenges, Appl. Energy 251 (2019), 113343, https://doi.org/10.1016/j.apenergy.2019.113343.
[8] T.L. Saaty, A scaling method for priorities in hierarchical structures, J. Math. Psychol. 15 (1977) 234–281, https://doi.org/10.1016/0022-2496(77)90033-5.
[9] T.L. Saaty, The Analytic Hierarchy Process: Planning, Priority Setting, Resources Allocation, McGraw-Hill, London, 1980.
[10] C. Kahraman, U. Cebeci, Z. Ulukan, Multi-criteria supplier selection using fuzzy AHP, Logist. Inf. Manag. 16 (2003) 382–394, https://doi.org/10.1108/09576050310503367.
[11] G.E. Gürcanli, U. Müngen, An occupational safety risk analysis method at construction sites using fuzzy sets, Int. J. Ind. Ergon. 39 (2009) 371–387, https://doi.org/10.1016/j.ergon.2008.10.006.
[12] M. Dağdeviren, İ. Yüksel, Developing a fuzzy analytic hierarchy process (AHP) model for behavior-based safety management, Inf. Sci. 178 (2008) 1717–1733, https://doi.org/10.1016/j.ins.2007.10.016 (Ny).
[13] Y. Wang, W. Yang, M. Li, X. Liu, Risk assessment of floor water inrush in coal mines based on secondary fuzzy comprehensive evaluation, Int. J. Rock Mech. Min. Sci. 52 (2012) 50–55, https://doi.org/10.1016/j.ijrmms.2012.03.006.
[14] A. Gnanavelbabu, P. Arunagiri, Ranking of MUDA using AHP and fuzzy AHP algorithm, Mater. Today Proc. 5 (2018) 13406–13412, https://doi.org/10.1016/j.matpr.2018.02.334.
[15] H.M. Lyu, W.H. Zhou, S.L. Shen, A.N. Zhou, Inundation risk assessment of metro system using AHP and TFN-AHP in Shenzhen, Sustain. Cities Soc. 56 (2020), 102103, https://doi.org/10.1016/j.scs.2020.102103.

[16] Y. Han, Z. Wang, X. Lu, B. Hu, Application of AHP to road selection, ISPRS Int. J. Geoinf. 9 (2020) 86, https://doi.org/10.3390/ijgi9020086.
[17] D.Y. Chang, Applications of the extent analysis method on fuzzy AHP, Eur. J. Oper. Res. 95 (1996) 649–655, https://doi.org/10.1016/0377-2217(95)00300-2.
[18] Z. Song, H. Zhu, G. Jia, C. He, Comprehensive evaluation on self-ignition risks of coal stockpiles using fuzzy AHP approaches, J. Loss Prev. Process Ind. 32 (2014) 78–94. 10.1016/j.jlp.2014.08.002.
[19] G. Zheng, N. Zhu, Z. Tian, Y. Chen, B. Sun, Application of a trapezoidal fuzzy AHP method for work safety evaluation and early warning rating of hot and humid environments, Saf. Sci. 50 (2012) 228–239, https://doi.org/10.1016/j.ssci.2011.08.042.
[20] P. Ping, D. Kong, J. Zhang, R. Wen, J. Wen, Characterization of behaviour and hazards of fire and deflagration for high-energy Li-ion cells by over-heating, J. Power Sources 398 (2018) 55–66, https://doi.org/10.1016/j.jpowsour.2018.07.044.
[21] C.Y. Jhu, Y.W. Wang, C.M. Shu, J.C. Chang, H.C. Wu, Thermal explosion hazards on 18650 lithium ion batteries with a VSP2 adiabatic calorimeter, J. Hazard. Mater. 192 (1) (2011) 99–107, https://doi.org/10.1016/j.jhazmat.2011.04.097.
[22] M. Chen, O. Dongxu, J. Liu, J. Wang, Investigation on thermal and fire propagation behaviors of multiple lithium-ion batteries within the package, Appl. Therm. Eng. 157 (2019), 113750, https://doi.org/10.1016/j.applthermaleng.2019.113750.
[23] S. Koch, K. Birke, R. Kuhn, Fast thermal runaway detection for lithium-ion cells in large scale traction batteries, Batteries 4 (2018) 16, https://doi.org/10.3390/batteries4020016.
[24] W..C. Chen, J..D. Li, C..M. Shu, Y..W. Wang, Effects of thermal hazard on 18650 lithium-ion battery under different states of charge, J. Therm. Anal. Calorim. 121 (2015) 525–531, https://doi.org/10.1007/s10973-015-4672-3.
[25] E. Ilbahar, A. Karaşan, S. Cebi, C. Kahraman, A novel approach to risk assessment for occupational health and safety using pythagorean fuzzy AHP & fuzzy inference system, Saf. Sci. 103 (2018) 124–136, https://doi.org/10.1016/j.ssci.2017.10.025.
[26] S. Chen, Z. Wang, W. Yan, J. Liu, Investigation of impact pressure during thermal runaway of lithium ion battery in a semi-closed space, Appl. Therm. Eng. 175 (2020), 115429, https://doi.org/10.1016/j.applthermaleng.2020.115429.
[27] S. Chen, Z. Wang, J. Wang, X. Tong, W. Yan, Lower explosion limit of the vented gases from Li-ion batteries thermal runaway in high temperature condition, J. Loss Prev. Process Ind. 63 (2020), 103992, https://doi.org/10.1016/j.jlp.2019.103992.
[28] S.C. Chen, Z.R. Wang, J.H. Liu, A novel quantitative analysis method on high temperature scope of jet fire and high-temperature mixture induced from a lithium-ion battery thermal runaway by infrared image technology, (2021), (Unpublished data, under review).
[29] S. Chen, Z. Wang, W. Yan, Identification and characteristic analysis of powder ejected from a lithium ion battery during thermal runaway at elevated temperatures, J. Hazard. Mater. 400 (2020), 123169, https://doi.org/10.1016/j.jhazmat.2020.123169.
[30] Y. Fu, S. Lu, K. Li, C. Liu, X. Cheng, H. Zhang, An experimental study on burning behaviors of 18650 lithium ion batteries using a cone calorimeter, J. Power Sources 273 (2015) 216–222, https://doi.org/10.1016/j.jpowsour.2014.09.039.
[31] J. Liu, Z. Wang, J. Gong, K. Liu, H. Wang, L. Guo, Experimental study of thermal runaway process of 18650 lithium-ion battery, Materials 10 (2017) 230, https://doi.org/10.3390/ma10030230 (Basel).
[32] D. Ouyang, M. Chen, J. Wang, Fire behaviors study on 18650 batteries pack using a cone-calorimeter, J. Therm. Anal. Calorim. 136 (2019) 2281–2294, https://doi.org/10.1007/s10973-018-7891-6.
[33] A.R. Baird, E.J. Archibald, K.C. Marr, O.A. Ezekoye, Explosion hazards from lithium-ion battery vent gas, J. Power Sources 446 (2020), 227257, https://doi.org/10.1016/j.jpowsour.2019.227257.
[34] W. Li, H. Wang, Y. Zhang, M. Ouyang, Flammability characteristics of the battery vent gas: a case of NCA and LFP lithium-ion batteries during external heating abuse, J. Energy Storage 24 (2019), 100775, https://doi.org/10.1016/j.est.2019.100775.
[35] A. Hammami, N. Raymond, M. Armand, Lithium-ion batteries: runaway risk of forming toxic compounds, Nature 424 (2003) 635–636, https://doi.org/10.1038/424635b.
[36] F. Larsson, P. Andersson, P. Blomqvist, B.E. Mellander, Toxic fluoride gas emissions from lithium-ion battery fires, Sci. Rep. 7 (2017) 10018, https://doi.org/10.1038/s41598-017-09784-z.
[37] J. Sun, J. Li, T. Zhou, K. Yang, S. Wei, N. Tang, N. Dang, H. Li, X. Qiu, L. Chen, Toxicity, a serious concern of thermal runaway from commercial Li-ion battery, Nano Energy 27 (2016) 313–319, https://doi.org/10.1016/j.nanoen.2016.06.031.
[38] GBZ230-2010, Classification for hazards of occupational exposure to toxicant, (2010), (In Chinese).